

Calculation of the Unstable Mixing Region in $\text{Zn}_{1-x}\text{Cd}_x\text{O}$ Ternary Alloys

I.I. SHTEPLIUK*

I. Frantsevich Institute for Problems of Material Science, NASU, 03680, Kiev, Ukraine

The $\text{Zn}_{1-x}\text{Cd}_x\text{O}$ ternary alloys with a narrow band gap, which are useful for light emitters in the visible wavelengths, are studied with respect to the unsteady region in mixing. This unstable region in mixing is calculated from the free energy of mixing using the strictly regular solution model. The interaction parameter used in this calculation is obtained by means of the valence-force-field model. An influence of the strain energy induced by substrate on the region of the spinodal decomposition for the $\text{Zn}_{1-x}\text{Cd}_x\text{O}$ system is studied and discussed.

DOI: [10.12693/APhysPolA.124.865](https://doi.org/10.12693/APhysPolA.124.865)

PACS: 64.75.-g, 81.30.-t, 81.30.Bx

1. Introduction

Wurtzitic $\text{Zn}_{1-x}\text{Cd}_x\text{O}$ ternary alloys and the structures with the lattice-matched $\text{Zn}_{1-x}\text{Cd}_x\text{O}/\text{ZnO}$ multiple quantum wells are extensively investigated because of applications for the light emitting diodes (LEDs) [1–7]. For this reason the study of the thermodynamic properties of the $\text{Zn}_{1-x}\text{Cd}_x\text{O}$ ternary alloy is very significant in the point of view of the fabrication of effective LEDs. It is important to clarify the miscible and the unstable composition of materials. The serious difference in the lattice periods and bond lengths of the wurtzitic ZnO and cubic CdO leads to the substantial strain energy of the $\text{Zn}_{1-x}\text{Cd}_x\text{O}$ ternary alloy. The strain energy enhances the internal energy of the alloy, thereby providing the tendency to decomposition. In other words, above-mentioned effect leads to an appearance of thermodynamically unsteady states. The phase separation of the unsteady states in semiconductor ternary alloys may be realized by the way of the spinodal decomposition. The spinodal decomposition gives rise to the formation of the nanodomains (or macroscopic phases) of different composition, lowering the internal energy of the alloy.

It should be noted that the effect of the spinodal decomposition on the optical efficiency of optoelectronic devices may be useful or harmful. The harmful effect is associated with the fact that the significant composition fluctuations in semiconductor alloys can cause the enlargement of the defect density (which may play a role of the non-radiative recombination centers) and lowering the performance of the LEDs. On the other hand, the spinodal decomposition could play a positive role. Earlier, it was proposed that the high luminescence efficiency of the InGaN-based LEDs could be related to the presence of In-rich regions in spite of the large defect density in the InGaN layers [8]. Above-mentioned

In-rich regions can act as In-rich quantum dots (QDs) in the InGaN layer, leading to appearance of deep potential wells that suppress the movement of carriers toward non-radiative recombination centers. In this case, the carrier localization within In-rich QDs has also a great effect on the quantum efficiency of LEDs, causing a large redshift in the emission energy and enhancement of the radiative recombination efficiency [9]. It was experimentally confirmed that the In-rich QDs in InGaN are generated by spinodal decomposition or phase separation [10]. Similar effects may also take place in $\text{Zn}_{1-x}\text{Cd}_x\text{O}$ ternary alloy that is the semiconductor analogue of the InGaN alloy. In addition, it was previously reported [11] that the InGaN films with a high structural quality were characterized by the homogeneous distribution of indium. Kret et al. [11] have found a very high quality of the multiple quantum wells with lateral indium fluctuations no higher than $\Delta x_L = 0.025$.

In this paper, the calculated unstable region of the $\text{Zn}_{1-x}\text{Cd}_x\text{O}$ system is reported. The strictly regular solution model is used for the calculation of the free energy of ternary alloy. The phase diagram is calculated from the free energy of mixing. The theoretical study of the strain energy effect on the thermodynamic properties of $\text{Zn}_{1-x}\text{Cd}_x\text{O}$ ternary alloy is also presented.

2. Theoretical approach

It should be mentioned that the thermodynamic properties of $\text{Zn}_{1-x}\text{Cd}_x\text{O}$ may be determined using the phase diagram in the terms of regular-solution model [12–14]. In the case of alloys, the Gibbs free energy of mixing, ΔG_m , can be expressed as

$$\Delta G_m = \Delta H_m - T\Delta S_m, \quad (1)$$

where

$$\Delta H_m = \Omega x(1-x), \quad (2)$$

$$\Delta S_m = -R[x \ln x + (1-x) \ln(1-x)]. \quad (3)$$

ΔH_m and ΔS_m are the enthalpy and entropy of mixing, respectively. Ω is the interaction parameter which depends on the material, R is the gas constant and T is

*e-mail: shtepliuk_1987@ukr.net

the absolute temperature. The choice of the interaction parameter was carried out from data obtained by the valence-force-field model (VFF-model) [15, 16]. In accordance with this model, the interaction parameter can be expressed as

$$\Omega = 1.74 \times 10^6 \left(\frac{\Delta a}{a_{ave}} \right)^{2.45}, \quad (4)$$

where Δa is the difference in lattice parameters for components of the solution ($\Delta a = a_{ZnO} - a_{CdO}$) and a_{ave} is the average value of lattice parameters for components ($a_{ave} = (a_{ZnO} + a_{CdO})/2$). In the approximation of the strictly regular solution, the interaction parameter does not depend on both the temperature and the composition. For the $Zn_{1-x}Cd_xO$ ternary alloy the total excess free energy ΔG^{tot} can be given as

$$\Delta G^{tot} = \Delta G^m + \Delta G^{strain}, \quad (5)$$

where ΔG^{strain} is the strain energy induced by the substrate. For the calculation of the strain energy, the method was used which was developed on the basis of the elastic model by Nakajima et al. [17, 18]. Nakajima proposed the approach for the calculation of the precise stress distribution of heterostructure. In this method, each component layer is broken down into many imaginary thin layers [17], and the face force and strain balance are considered over all these thin layers with coherent interfaces. In this case, the strain energy ΔG^{strain} is given by

$$\Delta G^{strain} = \sum_{i=1}^m U_i = \sum_{i=1}^m \frac{\alpha A_i d_i \sigma_i^2}{2E_i}, \quad (6)$$

where U_i is the elastic strain energy in the i -th fictitious thin layer, m is the total number of fictitious thin layers, σ , E_i , A_i , and d_i are the stress, Young modulus, surface area and thickness of the i -th fictitious thin layer. The strain energy per mole was obtained using the following parameter: $\alpha = 1/L$, where L is the layer thickness, which can be expressed by the number of lattice layers. For calculations, the parameter of $\alpha = 0.005$ was used. The parameter of $\alpha = 0.005$ means that the layer thickness is 200 lattice layers. When the thickness of the fictitious thin layer is one lattice-layer, A_i can be written as follows:

$$A_i = \frac{1}{2} \frac{\sqrt{3} N_A a_i^2}{4}, \quad (7)$$

where a_i is the lattice constant of the i -th fictitious thin layer. The parameters for the calculations were extracted from previous works [1–6].

3. Results and discussion

The free energy of mixing, ΔG_m , was accurately calculated using Eqs. (1)–(4). Figure 1 shows the free energy of mixing for the $Zn_{1-x}Cd_xO$ alloy versus composition x at several selected temperatures. The dependences of the free energy on the composition demonstrate two minima in place of just one. The presence of two minima is a sign that for a range of compositions (between these

two minima) two phases with the similar structure but diverse compositions are in equilibrium. There exists a region between these two minima where the curvature of the free energy ($\partial^2 G_m / \partial x^2$) is less than zero (the locus of points at which $\partial^2 G_m / \partial x^2 = 0$ at different temperatures determines the spinodal on the phase diagram). These results were used to calculate the T - x phase diagram.

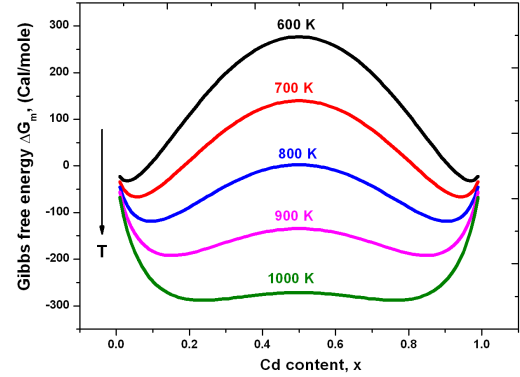


Fig. 1. Mixing free energy (ΔG_m) of $Zn_{1-x}Cd_xO$ alloy as a function of composition x for different temperatures.

In order to know the effect of the strain energy on the calculation of the phase diagram, this energy was calculated by means of Eqs. (5)–(7) for the $Zn_{1-x}Cd_xO/ZnO$ structure. The corresponding phase diagram was determined. Figure 2 shows the dependence of the strain energy per mole of $Zn_{1-x}Cd_xO/ZnO$ structure as a function of the cadmium fraction x . The strain energy rises as the composition of cadmium increases.

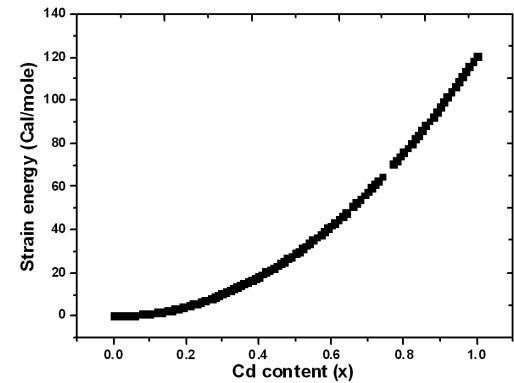


Fig. 2. The strain energy per mole of $Zn_{1-x}Cd_xO/ZnO$ structure as a function of the Cd fraction x in the $Zn_{1-x}Cd_xO$ solution.

When the strain effects are introduced, ΔG^{tot} in Fig. 3 exhibits pronounced two minima in the entire range of the alloy composition. However, dependences of the total excess free energy on the Cd content become asymmetric due to strain energy induced by the substrate. The T - x phase diagram undergoes some change. Spinodal decom-

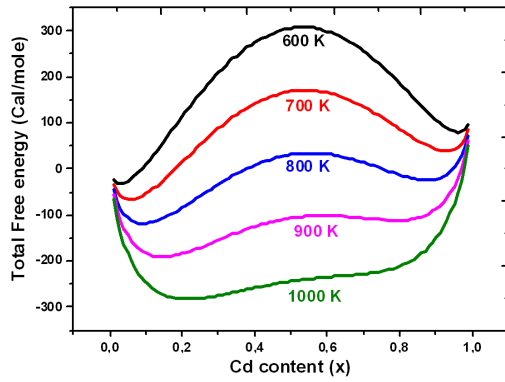


Fig. 3. Total excess free energy (ΔG^{tot}) of strained $\text{Zn}_{1-x}\text{Cd}_x\text{O}$ alloys grown on ZnO buffer as a function of composition x for different temperatures.

position taking place in unstrained samples is predicted to be suppressed in the samples under strain.

Figure 4 shows the calculated phase diagram, including the spinodal curves for the unstrained and strained $\text{Zn}_{1-x}\text{Cd}_x\text{O}$ alloys. The symmetry of obtained phase diagrams is caused by the use of Ω as x -independent, which is similar to the qualitative behavior of other alloys [19]. The spinodal line in the phase diagram designates the equilibrium solubility limit (the miscibility gap). For temperatures and compositions above this curve, a homogeneous alloy is predicted. There was observed a critical temperature T_C of 1140 K for unstrained $\text{Zn}_{1-x}\text{Cd}_x\text{O}$ ternary alloy. This result indicates that the $\text{Zn}_{1-x}\text{Cd}_x\text{O}$ alloy is stable at the high temperature. However, certain changes occur for strained alloys. In the case of ZnO substrate with lattice constant smaller than that of $\text{Zn}_{1-x}\text{Cd}_x\text{O}$, the critical temperature is reduced by about 62 K ($T_C \approx 1078$ K). Simultaneously, the miscibility gap and the region of spontaneous decomposition are diminished. The value of T_C , obtained in this study for strained ternary alloy, is contrast to results of Schleife et al. [20], which reported about critical temperature of 1030 K for $\text{Zn}_{1-x}\text{Cd}_x\text{O}$ solid solution. Nevertheless, similar results were reported by Karpov [21]. This author calculated the critical temperatures of the strained and relaxed $\text{In}_x\text{Ga}_{1-x}\text{N}$ layers using modified VFF model [21]. According to the calculation of Karpov [21], the elastic strain in an $\text{In}_x\text{Ga}_{1-x}\text{N}$ layer lowers the critical temperature.

For typical growth temperatures for $\text{Zn}_{1-x}\text{Cd}_x\text{O}$ (793 K [22] and 923 K [23]), phase separation for a wide range of compositions was observed. For these temperatures, the phase diagram shown in Fig. 4 indicates that there is spinodal decomposition in the interval of $0.229 \leq x \leq 0.768$ for growth temperature of 793 K, and in the interval of $0.286 \leq x \leq 0.711$ for growth temperature of 923 K. This is consistent with experimental findings, and explains why successful growth of these $\text{Zn}_{1-x}\text{Cd}_x\text{O}$ alloys without phase separation is achieved only for very small Cd contents, $x = 0.02$ for growth tem-

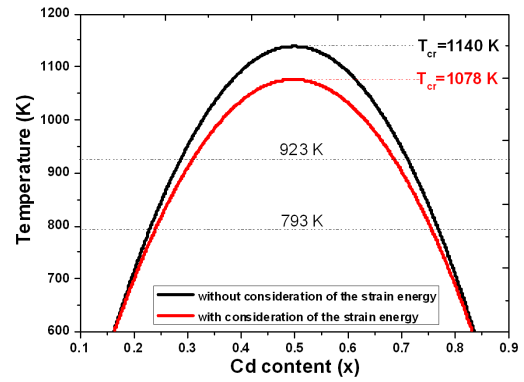


Fig. 4. Phase diagrams (T - x) for the unstrained and strained $\text{Zn}_{1-x}\text{Cd}_x\text{O}$ ternary alloys.

perature of 793 K [22]. Nevertheless, other experimental results devoted to studies of the solid solubility of cadmium in wurtzitic ZnO were reported. For example, Ishihara et al. [24] reported that the single phase $\text{Zn}_{1-x}\text{Cd}_x\text{O}$ solid solutions with cadmium solubility of 69 at. % may be grown by means of metal organic chemical vapor deposition (MOCVD) technique. These authors have explained such great value of solid solubility by the fact that the crystal growth under extremely non-equilibrium condition becomes indispensable to alloy with a wurtzite ZnO and a rock-salt CdO without the phase separation.

Additionally, it should be mentioned that the biaxial strain (caused by misfit between the film and the substrate) can be extremely important for the thermodynamic behavior of the $\text{Zn}_{1-x}\text{Cd}_x\text{O}$ alloys [25]. Indeed, the region of spontaneous decomposition at typical growth temperatures may be reduced and Cd solubility limit may be significantly increased. Phase separation suppression due to biaxial strain was also reported for InGaN epitaxial layers [26]. Earlier, it was reported that the type of the substrate does affect the average Cd incorporation into ZnO films [6]. A certain type of the substrate, depending on the provided in-plane strain — tensile or compressive, may promote or prevent the impurity incorporation. Obtained experimental findings could be associated with changes of the thermodynamics of the film growth.

In this study, it was revealed that the region of the spinodal decomposition is diminished due to the strain effect. For the strained ternary alloy, the phase diagram depicted in Fig. 4 suggests that there is spinodal decomposition in the range of $0.240 \leq x \leq 0.755$ for growth temperature of 793 K, and in the interval of $0.308 \leq x \leq 0.686$ for growth temperature of 923 K. Therefore, the choice of the optimal growth interface may be a key factor for the $\text{Zn}_{1-x}\text{Cd}_x\text{O}$ films without either phase separation or spinodal decomposition.

Hopefully these results will excite other experimental investigations and open the new ways for controlling the spinodal decomposition in $\text{Zn}_{1-x}\text{Cd}_x\text{O}$ ternary alloys.

4. Conclusions

Summarizing, the unstable mixing regions for the $\text{Zn}_{1-x}\text{Cd}_x\text{O}$ ternary alloys were predicted based on the strictly solution model. The interaction parameter used in this model was analytically obtained in terms of the valence force field model. It was found that the critical temperature for $\text{Zn}_{1-x}\text{Cd}_x\text{O}$ system was about 1140 K, which resulted in broad miscibility gap and led to a wide range of phase separation for typical growth temperatures. It was demonstrated that the strain energy can be extremely important for the thermodynamic behavior of the $\text{Zn}_{1-x}\text{Cd}_x\text{O}$ alloys. In general, the strain energy lowers the critical temperature by 62 K and reduces the region of spontaneous decomposition at typical growth temperatures.

References

- [1] I. Shtepliuk, G. Lashkarev, O. Khyzhun, B. Kowalski, A. Reszka, V. Khomyak, V. Lazorenko, I. Timofeeva, *Acta Phys. Pol. A* **120**, 500 (2011).
- [2] I. Shtepliuk, G. Lashkarev, V. Khomyak, P. Marianchuk, P. Koreniuk, D. Myroniuk, V. Lazorenko, I. Timofeeva, *Acta Phys. Pol. A* **120**, A61 (2012).
- [3] I. Shtepliuk, O. Khyzhun, G. Lashkarev, V. Khomyak, V. Lazorenko, *Acta Phys. Pol. A* **122**, 1036 (2012).
- [4] I. Shtepliuk, G. Lashkarev, V. Khomyak, O. Lytvyn, P. Marianchuk, I. Timofeeva, A. Ievtushenko, V. Lazorenko, *Thin Solid Films* **520**, 4772 (2012).
- [5] I. Shtepliuk, V. Khranovskyy, G. Lashkarev, V. Khomyak, V. Lazorenko, A. Ievtushenko, M. Syväjärvi, V. Jokubavicius, R. Yakimova, *Solid State Electron.* **81**, 72 (2013).
- [6] I. Shtepliuk, V. Khranovskyy, G. Lashkarev, V. Khomyak, A. Ievtushenko, V. Tkach, V. Lazorenko, I. Timofeeva, R. Yakimova, *Appl. Surf. Sci.* **276**, 550 (2013).
- [7] S. Sadofev, S. Kalusniak, J. Puls, P. Schäfer, S. Blumstengel, F. Henneberger, *Appl. Phys. Lett.* **91**, 231103 (2007).
- [8] Y. Narukawa, Y. Kawakami, M. Funato, S. Fujita, S. Fujita, S. Nakamura, *Appl. Phys. Lett.* **70**, 981 (1997).
- [9] C.A. Tran, R.F. Karlicek, Jr., M. Schurman, A. Osinsky, V. Merai, Y. Li, I. Eliashevich, M.G. Brown, J. Nering, I. Fergerson, R. Stall, *J. Cryst. Growth* **195**, 397 (1998).
- [10] I.-K. Park, M.-K. Kwon, S.-H. Baek, Y.-W. Ok, T.-Y. Seong, S.-J. Park, *Appl. Phys. Lett.* **87**, 061906 (2005).
- [11] S. Kret, P. Dłużewski, A. Szczepańska, M. Żak, R. Czernecki, M. Kryśko, M. Leszczyński, G. Maciejewski, *Nanotechnol.* **18**, 465707 (2007).
- [12] R.A. Swalin, *Thermodynamics of Solids*, Wiley, New York 1961.
- [13] L.G. Ferreira, S.H. Wei, J.E. Bernard, A. Zunger, *Phys. Rev. B* **40**, 3197 (1999).
- [14] L.K. Teles, J. Furthmüller, L.M.R. Scolfaro, J.R. Leite, F. Bechstedt, *Phys. Rev. B* **62**, 2475 (2000).
- [15] T. Takayama, M. Yuri, K. Iton, T. Baba, J.S. Harris, Jr., *Jpn. J. Appl. Phys.* **39**, 5057 (2000).
- [16] T. Takayama, M. Yuri, K. Iton, T. Baba, J.S. Harris, Jr., *J. Cryst. Growth* **222**, 29 (2001).
- [17] K. Nakajima, *J. Cryst. Growth* **121**, 278 (1992).
- [18] K. Nakajima, K. Furuya, *Jpn. J. Appl. Phys.* **33**, 1420 (1994).
- [19] M. Ferhat, F. Bechstedt, *Phys. Rev. B* **65**, 75213 (2002).
- [20] A. Schleife, M. Eisenacher, C. Rodl, F. Fuchs, J. Furthmüller, F. Bechstedt, *Phys. Rev. B* **81**, 245210 (2010).
- [21] S.Yu. Karpov, *MRS Internet J. Nitride Semicond. Res.* **3**, 16 (1998).
- [22] V. Venkatachalapathy, A. Galeckas, M. Trunk, T. Zhang, A. Azarov, A. Kuznetsov, *Phys. Rev. B* **83**, 125315 (2011).
- [23] K. Yamamoto, T. Tsuboi, T. Ohashi, T. Tawara, H. Gotoh, A. Nakamura, J. Temmyo, *J. Cryst. Growth* **312**, 1703 (2010).
- [24] J. Ishihara, A. Nakamura, S. Shigemori, T. Aoki, J. Temmyo, *J. Appl. Phys. Lett.* **89**, 091914 (2006).
- [25] O.S. Emeljanova, S.S. Strelchenko, M.P. Usacheva, *J. Semicond.* **43**, 135 (2009).
- [26] A. Tabata, L.K. Teles, L.M.R. Scolfaro, J.R. Leite, A. Khartchenko, T. Frey, D.J. As, D. Schikora, K. Lischka, J. Furthmüller, F. Bechstedt, *Appl. Phys. Lett.* **80**, 769 (2002).